140-year daily ensemble streamflow reconstructions over 661 catchments in France

Alexandre Devers[1], Jean-Philippe Vidal[2], Claire Lauvernet[2], Olivier Vannier[3], and Laurie Caillouet[3]

[1]EDF-DTG, 134 Chem. de l'Étang, 38950 Saint-Martin-le-Vinoux, France
[2]INRAE, UR RiverLy, 5 rue de la Doua, CS 20244, 69625 Villeurbanne Cedex, France
[3]Compagnie Nationale du Rhône (CNR), 2 rue André Bonin, 69004 Lyon, France

Correspondence: Alexandre Devers (alexandre.devers@edf.fr)

Abstract. The recent development of the FYRE climate (French Hydroclimate REanalysis), a high-resolution ensemble daily reanalysis of precipitation and temperature covering the period 1871-2012 and the whole of France, offers the opportunity to derive streamflow series over the country from 1871 onwards. The FYRE Climate dataset has been used as input for hydrological modelling over a large sample of 661 near-natural French catchments using the GR6J lumped conceptual model.

5 This approach led to the creation of the 25-member hydrological reconstructions HyDRE spanning the 1871-2012 period. Two sources of uncertainties have been taken into account : (1) the climate uncertainty by using forcings from all 25 ensemble members provided by FYRE Climate, and (2) the streamflow measurement error by perturbing observations used during the calibration. The hydrological model error based on the relative discrepancies between observed and simulated streamflow has been further added to derive the HydREM streamflow reconstructions. These two reconstructions are compared to other hydro-

10 logical reconstruction with different meteorological inputs, hydrological reconstructions from machine learning algorithm and independent/dependent observations. Overall the results show the added value of the HydRE and HydREM reconstructions in terms of quality, uncertainty estimation, and representation of extremes, therefore allowing to better understand the variability of past hydrology over France.

1 Introduction

15 Long time series of streamflow observations allow to better apprehend the effect of current changes on hydrology and to challenge our water management against ancient extreme events such as low-flows or floods (Slivinski, 2018). However, even in a data-rich country such as France, the network of observations available before the 1970s is quite sparse (Caillouet et al., 2017). The use of the sole observed-based information can lead to hazardous extrapolation of trends (Giuntoli et al., 2013) or a truncate vision of past extreme events. Furthermore, multidecadal variations have been observed on the few records available of

20 streamflow (Bonnet et al., 2020, 2017; Boé and Habets, 2014), or on variables closely related to such as precipitation (Willems, 2013; Slonosky, 2002) showing the interest of long term reconstructions.

Another way to obtain long time series of streamflow is to make use of a hydrological model (see for example Brigode et al., 2016; Crooks and Kay, 2015; Smith et al., 2019). However, this approach requires long-term climatic information based on observations, downscaled global climate models/reanalysis, regional climate models or surface reanalyses. Over France, several

25   studies have already used this approach to reconstruct long-term streamflow time series (Caillouet et al., 2017; Kuentz et al., 2015; Dayon et al., 2015; Bonnet et al., 2017, 2020). Those studies mainly use, as forcings for hydrological models, climate reconstructions based on dowscaling of large-scale reanalyses spanning the entire twentieth century, such as the Twentieth Century Reanalysis (Compo et al., 2011) and the European Reanalysis of the Twentieth Century (Poli et al., 2016). Some of the climate reconstructions also integrate information from long-term observed time series to constrain the statistical downscaling

30   methodology (Kuentz et al., 2015; Bonnet et al., 2017, 2020). However, most of these studies do not provide any uncertainty on the result and/or do not integrate all the available in-situ observations.

To make up for those shortcomings, the FYRE Climate reanalysis (French HYdrometeorological REanalysis, Devers et al., 2020a, 2021), a high-resolution 25-member ensemble daily reanalysis of precipitation (Devers et al., 2020b) and temperature (Devers et al., 2020c) covering the period 1871-2012, has recently been produced. This new dataset originates from an offline

35   data assimilation scheme (Bhend et al., 2012) based on the widely used Ensemble Kalman filter (Evensen, 2003). The prior-ensemble, called SCOPE Climate (Spatially COherent Probabilistic Extension Climate, Caillouet et al., 2016, 2017, 2019) originates from a statistical downscaling of a the Twentieth Century Reanalysis (20CR, Compo et al., 2011). FYRE climate assimilates historical daily observations of precipitation and temperature from the Météo-France database.

This study proposes to make use of the new FYRE Climate reanalysis as forcings into the lumped continuous rainfall–runoff

40   GR6J (Pushpalatha, 2013) to create long-term hydrological reconstructions over a large set of near-natural catchments in France. The modeling methodology builds on the work of Caillouet et al. (2017) but additionally takes into account several sources of uncertainties: (1) the climate uncertainty by using forcings from all 25 ensemble members provided by FYRE Climate, (2) the streamflow measurement error by perturbing observations used during the calibration, and (3) the hydrological model error through a post-processing based on the relative discrepancies between observed and simulated streamflow (Bourgin

45   et al., 2014). The modeling methodology led to the creation of two 25-member reconstructions providing daily streamflow over a set of 661 near-natural French catchments over the 1871-2012 period:

- HydRE (Hydrological REconstruction) including sources of uncertainty (1) and (2),

- HydREM (Hydrological REconstruction with Model error) additionally including the uncertainty related to the hydrological model error.

50   The paper is organised as follows: Section 2 introduces the observed streamflow series, two reconstruction datasets based on the same hydrological model (Safran Hydro and SCOPE Hydro, Caillouet et al., 2017), as well as alternative and larger-scale reconstructions from Ghiggi et al. (2019a). Section 3 describes the hydrological modelling strategy, the calibration methodology, the definition of the model error, and the creation of the HydRE and HydREM hydrological reconstructions. Their validation through different comparisons is presented in Sect. 4 and detailed example uses of the reconstruction – the study

55   of an extreme flood event in 1890 and monthly records of high and low flows – are also shown. Finally, several points are discussed in Sect. 5 and conclusions are drawn in Sect. 6.

2 Hydrological data

2.1 Observed streamflow

For this study daily observed streamflows for different sets of catchments are extracted from the national HydroPortail[1] database
60 (Leleu et al., 2014), see Figure 1.

661 near-natural catchments

This selection of near-natural stream is taken from Caillouet et al. (2017) and was based on the long-term observations available
($>$ to 26 years) and the quality of data during low-flows. Observations on these catchments are used for calibration and valida-
tion. Among those, 20 stations with long-term data have been selected to validate further the different reconstructions. Finally, 3
65 catchments with contrasted hydroclimatic conditions and long-term observations (Ubaye@Barcelonnette, Aveyron@Laguépie
and Gave d'Oloron@Sainte-Marie) have been selected as case study stations.

The 4 main river catchments over France

The Loire@Montjean-sur-Loire, Rhône@Beaucaire, Seine@Poses and Garonne@Tonneins are also selected as their represent
about 60% of the french territory. Furthermore, the Seine@Paris is also extracted as the observations time series is longer
70 than in Seine@Poses and has been used to asses multidecadal variability (Bonnet et al., 2020). Even if no modeling is done
on these catchments, their observed streamflow time series are used to assess the long-term variability of the hydrological
reconstructions.

2.2 Safran Hydro

The previous reconstruction of streamflow over the 661 catchments mentioned in Section 2.1 have been produced by Cail-
75 louet et al. (2017) using the daily lumped continuous rainfall–runoff model GR6J (Génie Rural à 6 Paramètres Journaliers,
Pushpalatha, 2013) and the Safran meteorological reanalysis as input (Quintana-Segui et al., 2008; Vidal et al., 2010) . More
details about the model is provided in Section 3.1. The Safran reanalysis is based on a optimal interpolation scheme merging in
situ observations and a background coming from climatology, large-scale reanalysis or operational analyses. Safran provides
hourly gridded meteorological data – on a 8 km grid – over France for the 1958-2021 period and is updated annually. Daily
80 precipitation, temperature and Penman-Monteith reference evapotranspiration (Allen et al., 1998) over the 661 catchments of
the study were computed using mean hourly values of Safran over the 1 January 1958–29 December 2012 period. The GR6J
model was calibrated over the 1973–2006 period using the Kling-Gupta Efficiency (Gupta et al., 2009) on the squared root of
streamflow as objective function. The hydrological reconstruction obtained through the modeling using Safran and GR6J spans
the 1958-2012 period and produces a deterministic simulation of daily streamflow over the 661 stations (Caillouet et al., 2017).
85 This dataset – called Safran Hydro – will be used to asses the quality of the hydrological reconstructions produced in this study

---

[1]https://www.hydro.eaufrance.fr/
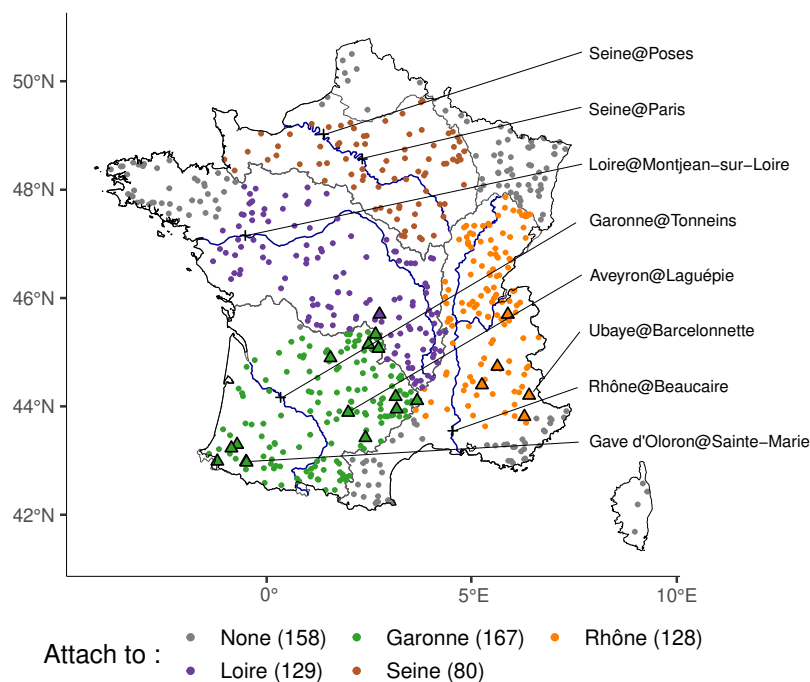
Figure 1. Location of the 661 outlets of the simulated catchments (circles and triangles) and of the 4 main rivers of France (crosses). Triangles indicate the outlets of the 20 catchments with the longest observational records. The three triangles with names indicate the case study catchments. Colors indicate the association between simulated catchments and the larger catchments of the 4 mains rivers of France based on the outlet location.

over the recent past. The Safran Hydro reconstruction is available through the Recherche Data Gouv platform (Caillouet et al., 2023a).

2.3 SCOPE Hydro

The GR6J model calibrated with the Safran reanalysis (see Section 2.2) have also been used with long-term climate reconstruc-
90 tion SCOPE Climate (Caillouet et al., 2019) as input (Caillouet et al., 2017). The SCOPE method (Caillouet et al., 2016, 2017) is based on the analog downscaling approach, i.e the hypothesis that similar large-scale patterns of atmospheric circulation lead to similar local meteorological conditions (Lorenz, 1969). The SCOPE Climate dataset consists of a daily 25-member ensemble reconstruction of precipitation (Caillouet et al., 2018a), temperature (Caillouet et al., 2018b), and Penman-Monteith reference evapotranspiration (Caillouet et al., 2018c) on the 8-km Safran grid. Data from SCOPE Climate were extracted
95 between 1 January 1871 and 29 December 2012, i.e the entire period of availability of SCOPE Climate, in order to compute catchment-average daily mean values over the 661 catchments. The hydrological reconstruction obtained through the modeling using SCOPE Climate and GR6J spans the 1871-2012 period and produces a 25-member ensemble daily streamflow recon-struction at the 661 stations (Caillouet et al., 2017). This dataset – called SCOPE Hydro – will be compared to the hydrological

reconstruction produced in this study over a long period of time (> 100 years). The SCOPE Climate reconstruction is available
100 through the Recherche Data Gouv platform (Caillouet et al., 2023b).

2.4 GRUN

The GRUN dataset (Ghiggi et al., 2019a) is a global gridded reconstruction of monthly runoff at 0.5°grid over the 1904-
2014 period. It is based on a machine learning algorithm trained during a recent period (Ghiggi et al., 2019b) with in-situ
streamflow observations of small catchments and uses precipitation and temperature from the Global Soil Wetness Project
105 Phase 3 (Kim et al., 2017) as predictors to reconstruct gridded monthly runoff. In order to account for uncertainty, the random
forest algorithm was trained on 50 subsets of data thus producing a 50-member ensemble in the reconstruction. Considering the
coarse resolution of the GRUN data, we can not compare it directly to the hydrological reconstructions at the 661 catchments.
Hence, GRUN values over the 1904-2012 period were extracted over the catchments of the 4 mains rivers of France in order
to compare long-term variability properties. Note that the Loire@Montjean-sur-Loire, Rhône@Beaucaire, Seine@Poses and
110 Garonne@Tonneins are composed of 106, 90, 73 and 75 cells in the GRUN dataset, respectively.

3 Methods

3.1 Hydrological model and snow module

The GR (Génie Rural) lumped continuous rainfall–runoff model are developed using a large number of catchments with
diversify hydroclimatic contexts and under the parsimonious principle, leading to a small number of parameters. Among the GR
115 models, GR5J and GR6J have already been used to produce daily long-term hydrological reconstructions (Brigode et al., 2016;
Caillouet et al., 2017). The GR6J daily lumped continuous hydrological model (Pushpalatha, 2013) is here used to provide the
hydrological reconstruction of this study, along with the snow module CemaNeige (Valéry et al., 2014). GR6J+CemaNeige
modelling were done with the AirGR package (Coron et al., 2017).

3.2 Meteorological forcings

120 The FYRE (French hYdrometerological REanalyis, Devers et al., 2021) Climate reanalysis is based on an offline Ensemble
Kalman filter (Evensen, 2003) called Ensemble Kalman fitting (Devers et al., 2021; Bhend et al., 2012; Franke et al., 2017).
It assimilates surface observations from Météo-France in to the daily SCOPE Climate reconstruction of temperature and pre-
cipitation. The data assimilation scheme has led to a daily 25-member ensemble available on the 8-km Safran grid over the
1871–2012 period for precipitation (Devers et al., 2020b) and temperature (Devers et al., 2020c). Data from FYRE Climate
125 were extracted between 1 January 1871 and 29 December 2012, i.e the entire period of availability of the climate reanalysis, in
order to compute the catchment-average daily mean over the 661 catchments. Note that since FYRE Climate does not provide
any estimation of the evapotranspiration, we used the Penman-Monteith reference evapotranspiration from SCOPE Climate
(Caillouet et al., 2018c) to complete the forcing datasets.

3.3 Calibration

130 3.3.1 Deterministic calibration

The combination of GR6J and CemaNeige requires the calibration of 8 parameters in total. In that respect we follow the work of Brigode et al. (2016) and Caillouet et al. (2017) :

- on the 176 catchments were the ratio snow/precipitation – computed using the Safran reanalysis – is higher than 10% the 8 parameters are calibrated freely,

135
- on the other catchments, the two parameters of CemaNeige are fixed to the median values from the previous 176 catchments. Thus only the 6 parameters of GR6J are calibrated.

This option has been retained as it allows the impact of a snow event to be simulated even in catchments where estimation of snow parameters was not possible due to a lack of snow events during the calibration period. However, using the mean of the 176 snow catchments represents a rough spatial extrapolation that could be improved by using a combination of co-variables, such as, for example the catchment's minimum and maximum elevation.

140 The criteria chosen for the calibration is the KGE (Gupta et al., 2009), as it allows understanding the quality of the reconstruction through is decomposition in correlation, bias and variability. The KGE is computed on the square root of streamflow in order to give similar weights to high and low flows. The calibration period is defined between 1 January 1973 and 30 September 2006 – following the work of (Caillouet et al., 2017) – in order to maximize the availability of observations. Finally,

145 the period between 1 January 1871 and 31 December 1972 is defined as a warm-up period.

3.3.2 Taking into account uncertainties in calibration

The calibration procedure described above is a deterministic one, i.e a unique time series of meteorological input and observation are provided to the model and the calibration led to a unique set of parameters. However, as mentioned in Section 3.2 the FYRE Climate reanalysis comes with uncertainty – noted ϵ_{meteo} – through a 25-member ensemble. The calibration procedure

150 was therefore applied separately for each of the 25-member in order to take that uncertainty into account.

Furthermore, the original calibration procedure considers perfect observations. However, estimating streamflow is not trivial and uncertainty arises from several sources (measurement devices, hydraulic conditions, number of gaugings). While some methods exist to evaluate properly this uncertainty (Le Coz et al., 2014), they require a lot of information which is clearly not available for each and every one of the 661 catchments. Hence, for this study we choose to define the observation error $- \epsilon_{obs}$

155 – on the daily streamflow through a simple gaussian distribution :

$$\epsilon_{obs} \sim \mathcal{N}(0, \sigma_{obs}) \tag{1}$$

with σ_{obs} equal to 15 % of the observed streamflow, following the work of Abaza et al. (2014) and Warrach-Sagi and Wulfmeyer (2010), and close to the one used in Clark et al. (2008) and Wongchuig et al. (2019). In order to include additionnal measure-

ment issues during low-flows, a minimum of σ_{obs}=0.01 mm/day is set. Twenty-five random perturbations were drawn each day
160   from ϵ_{obs} to create 25 observational time series.

In order to take into account the uncertainty of both FYRE Climate and streamflow observations, each member of FYRE Climate is randomly associated with a perturbed time series observations. We then applied the calibration procedure as described in Section 3.3.1 leading to the creation of 25 sets of parameters for each catchment.

3.4   Simulations

165   Simulations are conducted between 1 January 1871 and 29 December 2012. The year 1871 is repeated 3 times to account for the warm-up period of the model, following Caillouet et al. (2017). Given the relatively small size of the catchments, mostly less than 200 km2, and the lack of climate information prior to 1871, a 3-year warm-up period seems appropriate. Each of the 25 member of FYRE Climate is then randomly associated with one of the 25 sets of parameters obtained during the calibration step (see Section 3.3.2). Associations between a given FYRE Climate member and the parameter set derived from it were

170   avoided. To investigate the reduction in the number of members, two sets of simulations - one with all 625 associations and one with only 25 remaining in the final reconstructions - were compared on the 3 case study catchments (see Section 2.1) over the period 1973-2006. A Kolmogorov-Smirnov Two-Sample test was applied for each day. It showed that there is no significant difference between the distribution for the two samples at a significance level of 5% (not shown).

The simulations under FYRE Climate using the sets of parameters provided by the calibration (Section 3.3.2) therefore

175   produced a 25-member ensemble daily streamflow series at the 661 stations over the 1871-2012 period called HydRE (Hydrological REconstruction).

3.5   Definition and application of the error model

All the above methodology does not account for the error coming from the hydrological model. Indeed, even if the inputs and observations were perfect, a mismatch will still be present between the simulation and observations as the model is not a

180   perfect representation of the reality. This section describes the method used define the error model and how it is then applied on the newly created HydRE reconstruction.

3.5.1   From a deterministic methodology...

The error model $- \epsilon_{model} -$ is defined in a post-processing step using the residuals between the simulated and observed streamflow series, following a method developed in a forecasting context (Andréassian et al., 2007; Berthier, 2005; Bourgin

185   et al., 2014).

In the work of Berthier (2005) residuals (Res) are computed for each catchment over a defined period as follows:

$$Res = log(\frac{Q_{obs}}{Q_{sim}}) \tag{2}$$

with Q_{obs} observations and Q_{sim} a deterministic simulation.
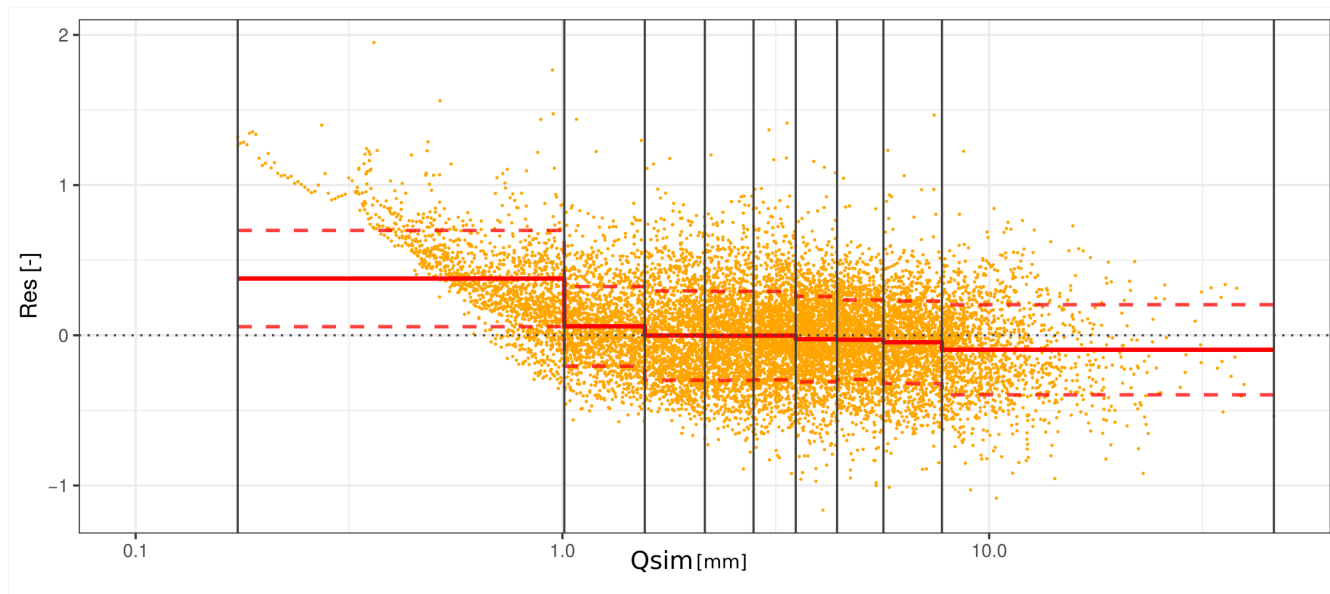
Figure 2. Example of the residuals (Res) values computed for the Ubaye@Barcelonnette between HydRE and the observations over the calibration period. The vertical lines represent the division of streamflow values in 9 classes. The solid (resp. dashed) red lines represent the mean (resp. standard deviation) of all residuals over each class. See Section 3.5 for details.

Residuals are then divided into 9 classes (index c) based on values of $Qsim$, each class having the same number of Res (see Figure 2). The objective is here to characterize the error model by taking into account the streamflow range (i.e high-flow or low-flow). For each class c we define the error model as a gaussian error:

$$\epsilon_{model}[c] \sim \mathcal{N}(\mu_{res}[c], \sigma_{res}[c]) \tag{3}$$

with $\mu_{res}[c]$ the mean and $\sigma_{res}[c]$ the standard deviation of Res belonging to the class c.

3.5.2 ... to a probabilistic methodology

However, the above methodology does account for neither the uncertainty in the observations nor the uncertainty in the simulation. In fact, a part of the $\epsilon_{res}[c]$ could be explained by the uncertainty in observations and in the simulation. As errors on observations and simulations have been already defined (Section 3.3.2 and Section 3.4) their influences can be removed from $\sigma_{res}[c]$.

We propose to replace Q_{sim} by the mean of the simulations $\overline{Q_{sim}}$ in Equation 2, leading to :

$$Res = log(\frac{Q_{obs}}{\overline{Q_{sim}}}) \tag{4}$$

and to modify the error model to account for different uncertainties:

$$\begin{cases} \mu_{model}[c] = \mu_{res}[c] \\ \sigma^2_{model}[c] = \sigma^2_{res}[c] - \sigma^2_{obs}[c] - \sigma^2_{Q_{sim}}[c] \end{cases} \tag{5}$$

with $\sigma_{Q_{sim}}$ the mean of the standard deviations computed on the ensemble simulated for the class c.

3.5.3 Computation

205   Q_{sim} simulations in Equation 4 and 5 were replaced by the HydRE reconstructions during the calibration period (see Sect. 3.4). If either $\overline{Q_{HydRE}}$ or Q_{obs} is below 0.01 mm/day, residuals are removed as Equation 4 could lead to high values. The definition of σ_{obs} is similar to the one used in the calibration methodology (see Section 3.3.2). Note that since the observation error is only roughly estimated, it is possible to find situations where $\sigma_{obs}[c] + \sigma_{ens}[c] > \sigma_{res}[c]$, but this only happens for 1.9% of the observations available over the 1973-2006 period. In that case the value of $\sigma_{obs}[c]$ is fixed to 0.01 mm.

210   3.5.4 Application

The error model defined above is then applied on the HydRE reconstruction. For each day and each member (m) a simulated streamflow $HydRE[m]$ belongs to a class c. One hundred error values – noted err – are drawn based on the model error:

$$err \sim \mathcal{N}(\mu_{model}[c], \sigma_{model}[c]) \tag{6}$$

The value of $HydRE[m]$ is then multiplied by the error value :

215   $$Q_{sim_{err}}[m] = HydRE[m] \times err \tag{7}$$

with $Q_{sim_{err}}[m]$ a vector of length 100.

Applying this methodology to the 25 members of HydRE leads to an ensemble of 2500 members (25 members $\times$ 100 errors). Among those 2500 members, 25 are randomly selected to retrieve a reasonable ensemble size while yet characterizing the uncertainty.

220   To investigate the reduction in the number of members, two sets of simulations - one with all 2500 members and one with only 25 members retained in the final reconstructions - were compared on the 3 case study catchments (see Section 2.1) over the period 1973-2006. A Kolmogorov-Smirnov test was applied between the 25-member and the 2500-member ensembles and confirmed the similarity of the distributions at the 0.05 level for 96.09% of the time for the Aveyron@Laguépie, 96.17% for the Gave d'Oleron@Sainte-Marie and 95.22% for the Ubaye@Barcelonnette.

225   Finally, the ensemble is reorganized to match the ranks of HydRE in order to preserve the spatio-temporal coherence lost through the random sampling. This method is applied each day over the 1871-2012 period on each of the 661 catchments and leads to a 25-member ensemble daily streamflow reconstruction called HydREM (Hydrological Reconstruction with Error Model).

3.6 Metrics

230 Several metrics are used to compare the different reconstructions. The Continuous Ranked Probability Score (Brown, 1974) is a commonly used score for ensemble verification and is defined as follow

$$CRPS[x,y] = \frac{1}{M} \sum_{i=1}^{M} \int_{-\infty}^{\infty} [F(x) - H(y)]^2 dx, \tag{8}$$

with x the ensemble to be evaluated, y the observation, F the cumulative distribution function, M the number of observations and H the Heaviside function. The decomposition of the CRPS (Hersbach, 2000) is also computed to study the reliability

235 part and the potential CRPS. As explained in Hersbach (2000) the reliability ($Reli$) gives an information similar to the rank histogram and the potential CRPS (Pot) is linked to the spread of the ensemble – the uncertainty – and to the number of outliers.

$$CRPS = Reli + Pot \tag{9}$$

The optimal value of the CRPS and its decomposition is then zero. Furthermore, in order to compare between the different

240 catchments the CRPS and it decomposition are normalized by the average streamflow over the 1976-2006 period. The normalized version of the scores is denoted with a N at the beginning ($NCRPS$,$NPot$,$NReli$) and are expressed as percentage of the average streamflow.

In addition, the KGE (Gupta et al., 2009) and his decomposition were used to provide a more insightful description of the datasets. The KGE is defined as follow :

245 $$KGE[x,y] = 1 - \sqrt{(r-1)^2 + (\alpha-1)^2 + (\beta-1)^2} \tag{10}$$

where r is the linear correlation coefficient, α the ratio of variance, and β the ratio of means. Contrary to the CRPS the optimal value of the KGE is 1 when the two vectors x and y match perfectly. KGE is computed for each ensemble member and median values over each ensemble are retained.

4 Results

250 This section presents an intercomparison of the two reconstructions developed here (HydRE and HydREM) and other products referred to in the previous sections: Safran Hydro (Sect. 2.2), SCOPE hydro (Sect. 2.3), and GRUN (Sect. 2.4). Such an intercomparison is performed on various aspects: (1) a daily time series example from 3 case study catchments, (2) comprehensive validation against observations over 1960-2012, (3) validation against the few long-term observations over 1920-2012, (4) assessment of multidecadal variations over the 4 main French basins, (5) long-term evolution of high-flow and low-flow events

255 at the monthly scale, and lastly (6) the example of an extreme flood event in 1890.
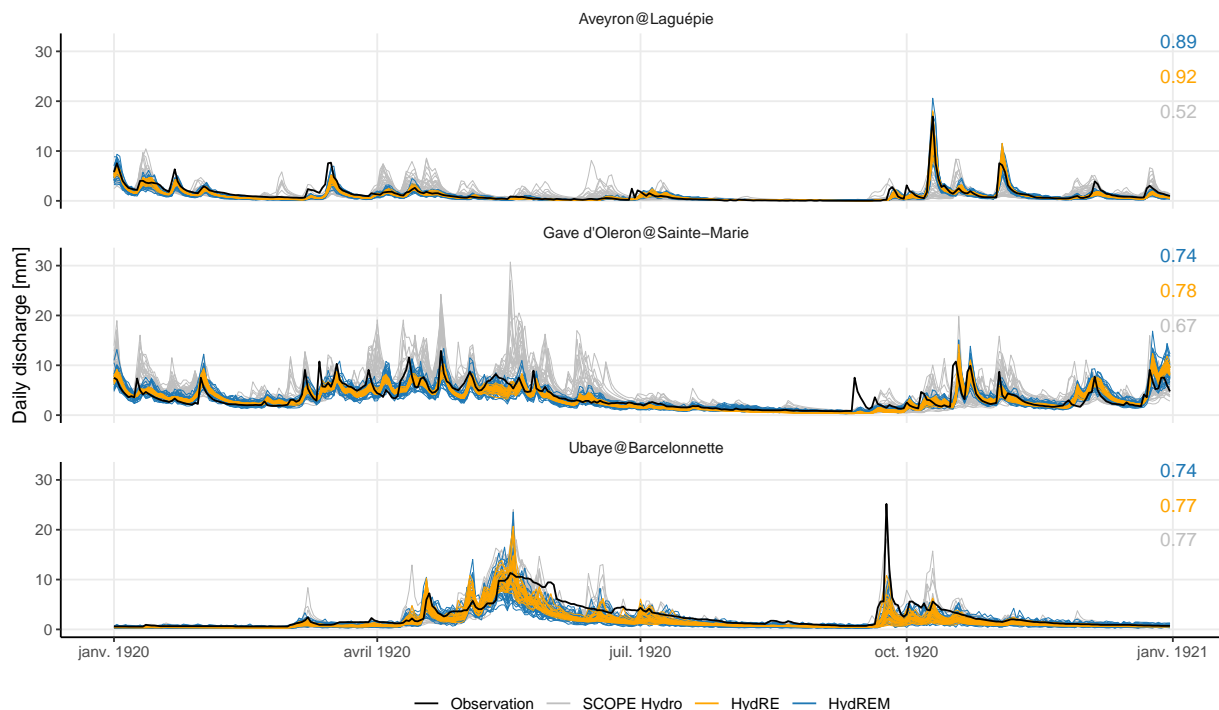
Figure 3. Daily time series over the 3 case study catchments during the year 1920. The values in the top-right corner indicate the median of the 25-correlations between the observation and the 25-member ensemble.

4.1 Time series example

A first assessment of the reconstructions is conducted through a daily time series analysis of the year 1920 for the three case study stations (Figure 3). This year is chosen to reflect the behaviour of the hydrological reconstructions in the distant past and because streamflow observations are available over the three stations. For SCOPE Hydro, the relatively high uncertainty

260   reflects the high uncertainty in SCOPE Climate – the coresponding meteorological input – as information only comes from a large-scale reanalysis. The uncertainty of HydRE is clearly lower as FYRE Climate used in-situ observations to reduce the uncertainty in the reanalysis. Finally, the HydREM uncertainty depends on the quality of FYRE Climate but also on the ability of GR6J to reproduce the hydrological behaviour of the catchment. For the Ubaye, the basin is influenced by snowmelt, which is quite difficult to reproduce, and the quality of the observations in 1920 is possibly flawed due to the management of

265   small upstream dams, as shown by the recession which seems unrealistic for some days. In any case, even while accounting for modeling error HydREM seems to have a lower uncertainty than SCOPE Hydro for Gave d'Oloron@Sainte-Marie and Aveyron@Laguépie. The ensemble of HydRE seems to be under-dispersed, but this is not the case once the modeling error from Sect. 3.5 is applied i.e in HydREM reconstructions. The added values of HydRE and HydREM, in comparison to SCOPE
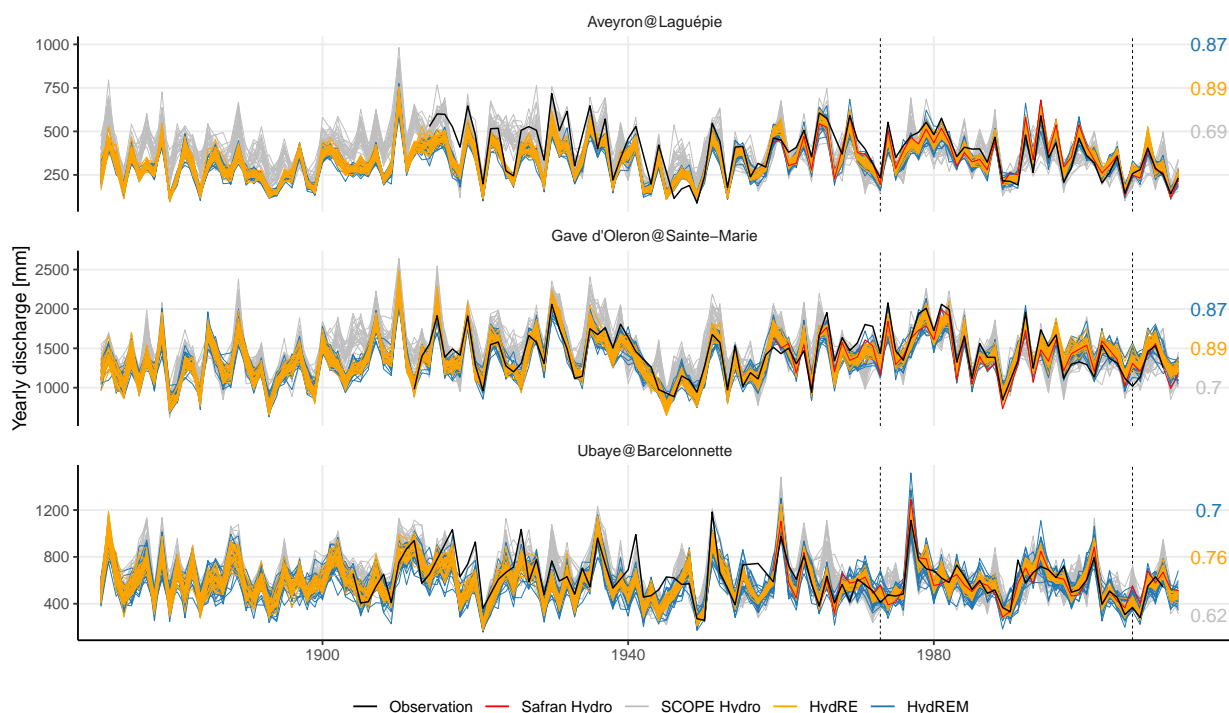
Figure 4. Yearly time series over the 3 case study catchments between 1871 and 2012. The values in the top-right corner indicate the median of the 25-correlations between the observation and the 25-member ensemble.

Hydro, in Gave d'Oleron@Sainte-Marie and Aveyron@Laguépie is clearly visible in terms of correlation with the observations.
However, for Ubaye@Barcelonette is is more difficult to find which of the reconstructions better reproduces the observations.

The time series of the three case study catchments are now investigated at a yearly time step (Figure 4). Over the 1960-2012 period, HydRE and HydREM show a higher correlation with observations than SCOPE Hydro. Furthermore, the uncertainty is lower in HydRE and HydREM than in SCOPE Hydro. HydRE and HydREM display a behaviour similar to Safran Hydro. However, the absence of uncertainty in Safran Hydro makes it difficult to compare to ensemble reconstructions. Before 1960, HydRE and HydREM still have a higher correlation with the observations than SCOPE Hydro.However, for Aveyron@Laguépie before 1940, a dry bias seems to appear in HydRE and HydREM which is not present in SCOPE Hydro. This could reflect a dry bias in the FYRE Climate reanalysis as it affects both HydRE and HydREM.

4.2 Validation against observations between 1960 and 2012

The performance of the different reconstructions is evaluated with the KGE during the calibration period 1976-2006 (Figure 5). SCOPE Hydro reconstruction shows the lowest KGE, which could be explained by the fact that (1) the reconstruction uses parameters calibrated with Safran and not SCOPE Climate, and (2) the meteorological forcing information comes only from a
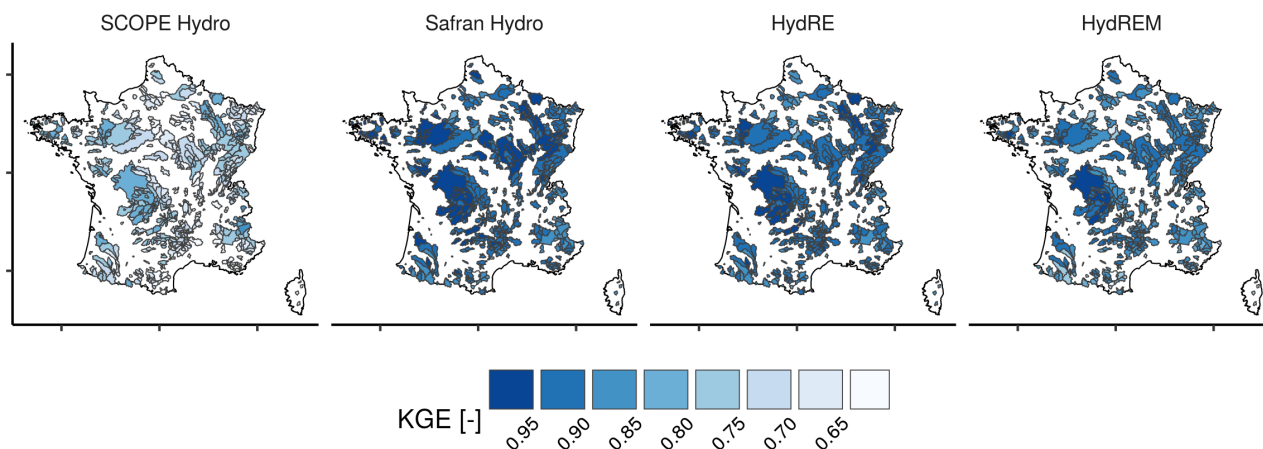
Figure 5. Map of the $\text{KGE}\left(\sqrt{Q}\right)$ computed during the calibration period for different hydrological reconstructions. For SCOPE Hydro, HydRE and HydREM the score is computed as the median of 25-member values.
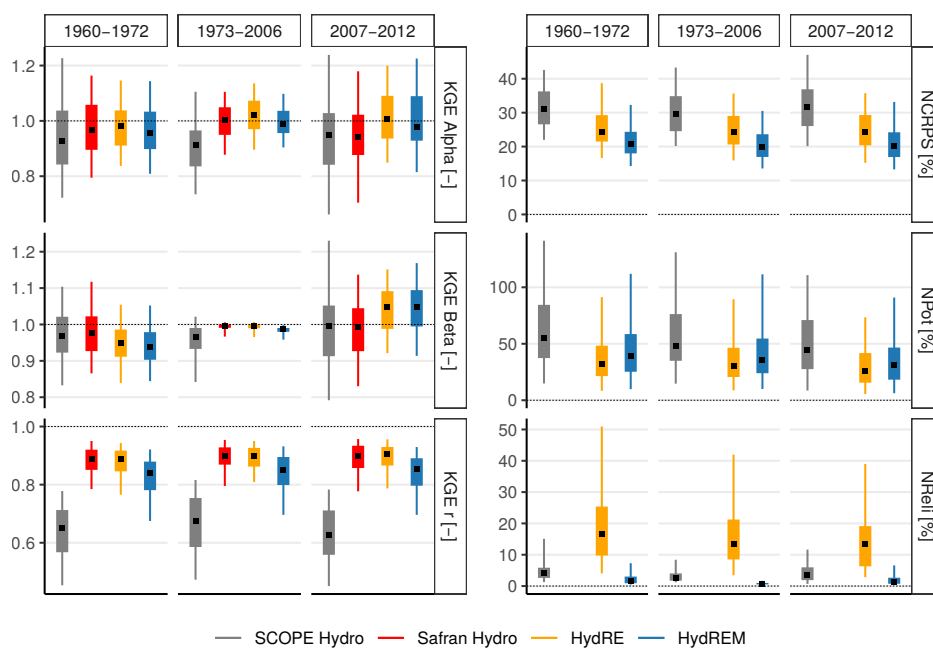
Figure 6. Boxplot of different metrics over 3 distinct periods using 173 stations. For SCOPE Hydro, HydRE and HydREM the score displayed is computed as the median of 25-member metrics. The square correspond to the median, the thick lines to the 25th and 75th quantiles and the narrow lines to the 5th and 95th quantiles. The black dotted lines represent the optimal values for each metrics.
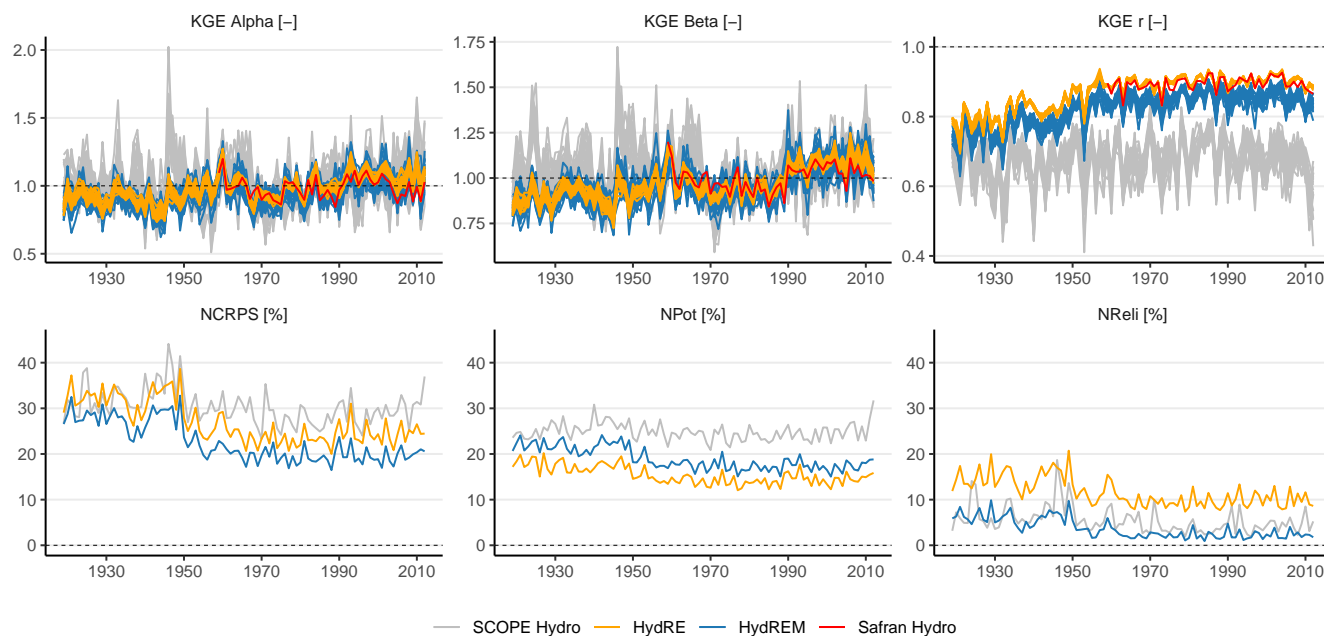
Figure 7. Evolution of metrics averaged over a set of 20 stations for the 1920-2012 period. For SCOPE Hydro, HydRE and HydREM the score is computed as the median of 25-member values. The black dotted lines represent the optimal values for each metrics. The NCRPS, NPot and NReli correspond respectively to the CRPS, Pot and Reli normalized by the averaged discharge at each station.

large-scale reanalysis. KGE values of Safran Hydro and HydRE are quite close, with some catchments showing slightly lower values in HydRE. This could be explained by the fact that HydRE values are medians over all 25 members. For HydREM, KGE values are slightly lower than in Safran and HydRE due to the application of random sampling and the increasing uncertainty

285   when the error model is applied.

To go further into the comparison over 1960-2012, we compute different metrics over three sub-periods : 1960-1972, 1973-2006 and 2007-2012. Metrics are computed only on 173 stations, i.e. the ones with observations available over the entire 1960-2012 period.

The decomposition of the KGE over the three sub-periods is shown in Fig. 6, left panels. Globally, the values of KGE Alpha

290   – the variability component – and KGE r – the correlation component – do not differ largely and the hierarchy between the different reconstructions is maintained over the different time periods. However, for the KGE Beta – the bias component – the values are closer to zero during the calibration period, except for SCOPE Hydro as it uses parameters calibrated with Safran. HydRE and HydREM exhibit a slight bias (+/ -5%) outside the calibration period in contrary to Safran Hydro. Overall, the KGE of SCOPE Hydro are sub-optimal in comparison to the other reconstructions. Safran Hydro, HydRE and HydREM show

295   almost similar values except for KGE r for which HydREM displays slightly lower values.
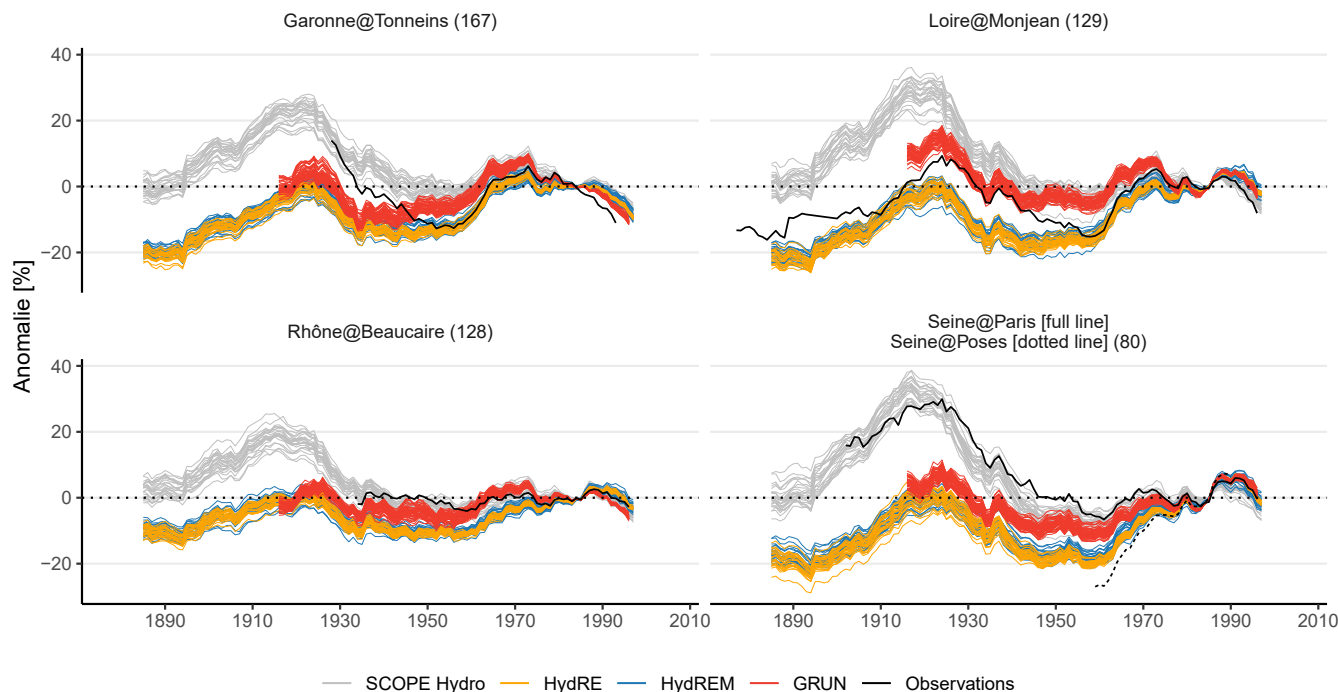
Figure 8. Multidecadal variations of different reconstructions over the 4 main catchments of France and comparison with available observation records. The number in brackets indicates the number of stations modeled in this catchment. See text for details.

The decomposition of the CRPS is also explored in Fig. 6, right panels. Note that it is not possible to compute the CRPS for the deterministic Safran Hydro reconstruction. As for the KGE, the hierarchy between the reconstructions are relatively stable over the three sub-periods for the different metrics. The NCRPS – the total CRPS relative to the mean streamflow over the calibration period – shows the advantage of using FYRE Climate as input, with lower values for HydRE and HydREM than for

300 SCOPE Hydro. Applying the error model also brings an improvement, although smaller, with lower values in HydREM. The NPot – part of the CRPS representing the accuracy – shows similar values between HydRE and HydREM showing no added value of the error model but lower values than SCOPE Hydro. In contrary, the NReli – related to the reliability of the ensemble – shows a under-dispersion of the HydRE ensemble with values much larger than for SCOPE Hydro or HydREM. Applyign the error model leads to a quite low (< 5%) NReli of HydREM and below the one of SCOPE Hydro.

305 The study among different time periods through the decomposition of KGE and CRPS shows the stability of HydRE and HydREM during the 1960-2012 period with results (1) close to Safran Hydro, (2) better than SCOPE Hydro, and (3) with a correct definition of the uncertainty for HydREM. However, it also shows a small bias outside the calibration period.

4.3 Validation against long-term observations over 1920-2012

This subsection looks further into the past in order to assess the quality of the hydrological reconstructions over the 1920-2012
310   period. Unfortunately before the 1970s the number of stations with continuous measurements decrease drastically. Therefore,
the twenty stations with the longest record of continuous observations, among the 661 near-natural catchments where discharge
was simulated, were selected here. While this set of 20 stations does not cover the entire hydro-climatic contexts in France –
they are mainly located in the south and in mountainous area (see Figure 1) – they allow a characterisation over a long time
period. The daily CRPS and its decomposition, as well as the KGE components, were computed for each year of the 1920-2012
315   period. This is done for each station and for deterministic metrics we compute the median values over the ensembles. Finally,
the average value over the 20 stations is computed and shown in Fig. 7.

As in Section 4.2, the CRPS decomposition shows the interest of HydRE and HydREM in terms of CRPS (NCRPS) and
potential CRPS (NPot) in comparison to SCOPE Hydro. However, the reliability (NReli) of HydRE is higher than the ones in
SCOPE Hydro and HydREM. Over time, both the potential CRPS and the reliability show first a plateau between 1920 and
320   1950, then a decrease over the 1950s and 1960s, and a new plateau until 2012. The transition period matches a strong increase
in the number of weather stations used in FYRE Climate (Devers et al., 2021). However, as this is also visible (although much
less) in SCOPE Hydro, this could be linked to another origin, see Section 5.

SCOPE Hydro display KGE Beta close to zero over the entire period but with a high dispersion. KGE Beta of HydRE
and HydREM are highly similar, with a small bias [+/-5%] during the 1960-2012 period and a dry bias centered around -
325   10% over the 1920-1950 period. Note that this is also the period identified in Sect. 4.1 at Aveyron@Laguépie. KGE Alpha
shows a behaviour similar to KGE Beta, with a high dispersion in SCOPE Hydro and good results for HydRE and HydREM,
but a variability lower in HydRE and HydREM than in the observations during 1920-1950. This could possibly explain the
bias appearing at the same time as underestimating variability could lead to underestimation of peak streamflow playing an
important role in yearly-averaged streamflow. For KGE r, even if HydREM displays slightly lower correlations than HydRE,
330   their values are always above the ones in SCOPE Hydro even at the beginning of the period. For HydRE and HydREM a strong
evolution is visible over the year linked to the number of observation assimilated in FYRE Climate (Devers et al., 2021).

As a summary, even if a small dry bias seems to appear before the 1950s, the HydREM reconstruction shows the added
values of both using a reanalysis as input and using a model error.

4.4 Multidecadal variations over large catchments

335   In order to further describe HydRE and HydREM, multidecadal variations in the reconstruction are compared to the ones in
SCOPE Hydro, in the observations over the 4 main rivers of France (see Section 2.1), and in the GRUN dataset (see Section 2.4).
As those products have different spatial and temporal resolutions, transformations are first applied:

–   For SCOPE Hydro, HydRE and HydREM, yearly anomalies are first computed over 1871-2012 with respect to the 1970-
2000 period for each of the 25 members and for the 661 catchments. Each simulated catchment is then assigned to one
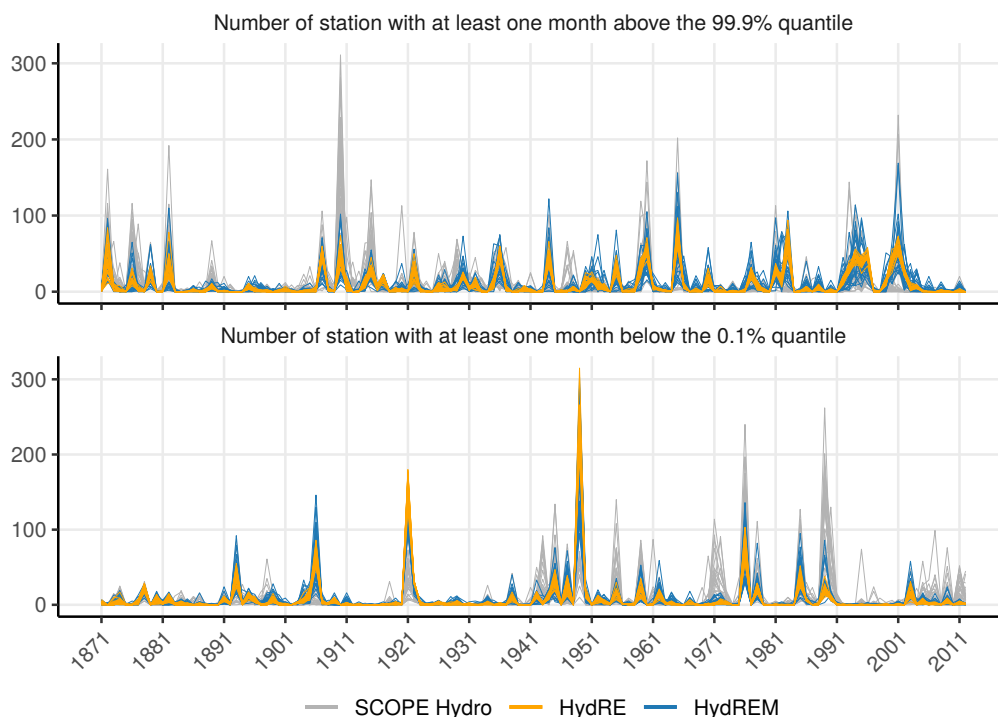
Figure 9. Evolution of the number of station with at least one monthly streamflow above (below) the 99.9% (0.1%) monthly quantile during a year. This is applied separately for each of the 25 member and the period of reference used to computed the quantile is 1871-2012.

340   of the main rivers (see Figure 1). Finally, for each member and main river, the mean of the all catchment anomalies is computed.

- – For GRUN, yearly anomalies over 1871-2012 in respect to the 1970-2000 period are computed for each grid cell over France for each of the 50 members. Each cell is then assigned to a main river based on its location (see Section 2.4 for the number of cells by catchments). As previously, for each member and main river, the average of grid cell anomalies
345   is computed.

- – For the observations, yearly anomalies over 1871-2012 in respect to the 1970-2000 period are simply computed for the four main rivers.

Finally, a 30-yr centered rolling mean is applied to each time series of anomalies to highlight multidecadal variations.

Results are presented in Fig. 8. First, applying the error model does not affect multidecadal variations as HydRE and Hy-
350   dREM display similar ones, even if the dispersion is different. Overall, the GRUN dataset is closer to the HydRE and HydREM reconstructions than to SCOPE Hydro, especially before 1940, except for the Loire@Montjean. Indeed, during the 1900-1940 period, SCOPE Hydro shows strong positive anomalies which are not shown by HydRE, HydREM, or GRUN.

Concerning the Garonne@Tonneis, the observations are closer to SCOPE Hydro than HydRE, HydREM or GRUN before
1950. For the Rhône@Beaucaire, multidecadal variations in the observations shows less variability than in the different re-

355 constructions, GRUN included. This could reflect the strong anthropogenic modifications of the Rhône catchment. For the
Seine@Poses, HydRE and HydREM are closer to the observations than SCOPE Hydro or GRUN over 1950-2012, but the time
series is rather short. For Seine@Paris, the observations are quite coherent with SCOPE Hydro over the whole period. The
other reconstructions do not provide coherent multidecadal variations. However, the catchments used to compare the varia-
tions in the reconstructions cover a larger area than the Seine@Paris catchment's. Lastly, for the Loire@Montjean, the GRUN

360 dataset seems to better represent observed variations. Indeed, over the 1920-1940 period, a overestimation is seen in SCOPE
Hydro whereas HydRE/HydREM underestimate anomalies. However, for HydRE/HydREM this tendency is almost null over
1890-1920 whereas it still present in SCOPE Hydro.

Globally, all hydrological reconstructions have difficulties in representing the multi-decadal variations present in the dis-
charge observations. The sources of these discrepancies are probably multiple and difficult to quantify, but several have been

365 identified: (1) observations from the distant past could be erroneous and the change in the system measurement could lead to
strong inhomogeneities (Kuentz et al., 2015), (2) the hydrological model could have difficulties in simulating the multidecadal
variability, but the discrepancies appear both in the reconstructions GRUN produced by a random forest algorithm and SCOPE
Hydro/HydRE/HydREM produced by GR6J an conceptual hydrological model, (3) the hydrological models do not provide
a discharge simulation at the hydrological station of the 4 main rivers, the time series are aggregated over a large catchment

370 and the anomalies are calculated subsequently, and (4) HydRE and HydREM, as suggested by Figure 7, are affected by a dry
before the 1940s that leads to a 'rising' trend in the anomalies (for SCOPE Hydro the inverse is visible).

4.5 Evolution of monthly high-flow and low-flow events over the 1871-2012 period

Figure 9 allows to grasp the evolution of the number of stations with at least one monthly streamflow above (below) the 99.9%
(0.1%) monthly quantile during a year.

375 For high-flows (Fig. 9, top panel), the methodology highlights different years with a large number of stations with monthly
values above the 99.9% quantile. Among them : 1872, 1876, 1882, 1907, 1910, 1935-1936, 1944-1945, 1954-1955, 1960-1961,
1966, 1993-1994 and 2001. The frequency of events does not seems to follow a clear tendency, but the 1885-1905 period shows
a quite low number of stations. It is important to note that all the years mentioned above are consistent with the ones available in
"Les inondations remarquables en France" (Lang and Coeur, 2014, "Remarkable Floods in France") which provides a thorough

380 review of floods over the 1770-2011 based on archive evidence.

Furthermore, one can also find some interesting references to those years in other literature sources and even paintings:

– winter 1872-1873 with the Seine flood as testified in Alfred Sisley's painting "Le Bac de l'île de la loge, inondation"
   ("The ferry of loge island, flooding"),

– the first months of 1910 are also largely documented in Lang and Coeur (2014) with flood occurring on the northern half

385   of France,

– the end of 1935 is also mentioned (Pardé, 1937; Lang and Coeur, 2014) with floods in the Seine and the Rhône rivers,

– winter 1954-1955 is also present with several floods for the Rhône river (Pardé, 1958) but also on the Seine river (Lang and Coeur, 2014). Furthermore, a slow flood also hit the Saône river, leading to a up to 6 km-wide river in some places (Dubrion, 2008).

390   Among the years with a relatively high number of stations with low-flows (Fig. 9, bottom panel), the year 1893 was already identified in Ireland and in the Uk by Cook et al. (2015). The year 1906 allow to identify the well know meteorological drought identified by Plumandon (1907). The 1921 drought event (Duband, 2010) is also well seen in the HydREM data set with a large temporal extent. Another long drought is see around the year 1949 which is also mentioned for the Loire catchment (Moreau, François, 2004). Finally, the droughts of 1976, 1985, 1990 and more recently 2003 are consistent with observation time series

395   showing record-breaking minimum for these years.

It is interesting to note that most of the events are captured in both SCOPE Hydro and HydRE/HydREM. This is actually not surprising given the monthly time step. Indeed, the added value of HydRE and HydREM comes from the assimilation of daily meteorological values in their input, i.e. with FYRE Climate. Still, some events seem more or less important when looking at SCOPE Hydro or HydRE/HydREM, e.g. high-flows in 1910 and low-flows in 1971 and 1990.

400   The study of the high-flows and low-flows records in HydRE and HydREM reconstructions shows the interest of such datasets to better apprehend extremes of the past, and a good coherence with other indirect sources of data.

4.6   Example of an extreme flood event

At the end of September 1890, an extreme rainfall event in the Cévennes area, in Southern France [2] led to a record flood over the Ardèche river between 21 and 23 September 1890 (Sheffer et al., 2003; Naulet et al., 2005). Daily streamflow between

405   20 and 25 September were transformed into quantiles with respect to the entire 1871-2012 period, independently for each reconstruction dataset (SCOPE Hydro, HydRE, and HydREM) and each member. The mean of the 25 quantiles – one for each member – are displayed in Figure 10. Only few observations are available in the Cévennes and the stations are located in the east-part of the region where the event was less important. We choose not to display those observations because the short period of observation does not allow to comput long term quantiles such as those used in the reconstructions.

410   SCOPE Hydro first demonstrate low quantiles values over all catchments compared to HydRE/HydREM. Indeed, only a few members in SCOPE Hydro display high values (not shown) but this does not affect the mean of the ensemble. The mean values in HydRE and HydREM are more coherent with the studies mentioned above than the one in SCOPE Hydro given the exceptional nature of the event. Furthermore, HydRE and HydREM show a spatial structure coherent with the events usually observed in the Cévennes area with vary high values on a small number of catchments. Finally, the difference between HydRE

415   and HydREM on some catchments shows the sensitivity of the model error regarding the high-range streamflow simulated.

---

[2]http://pluiesextremes.meteo.fr/france-metropole/Inondations-en-Cevennes-Crue-historique-de-l-Ardeche.html, last access: 21 February 2022
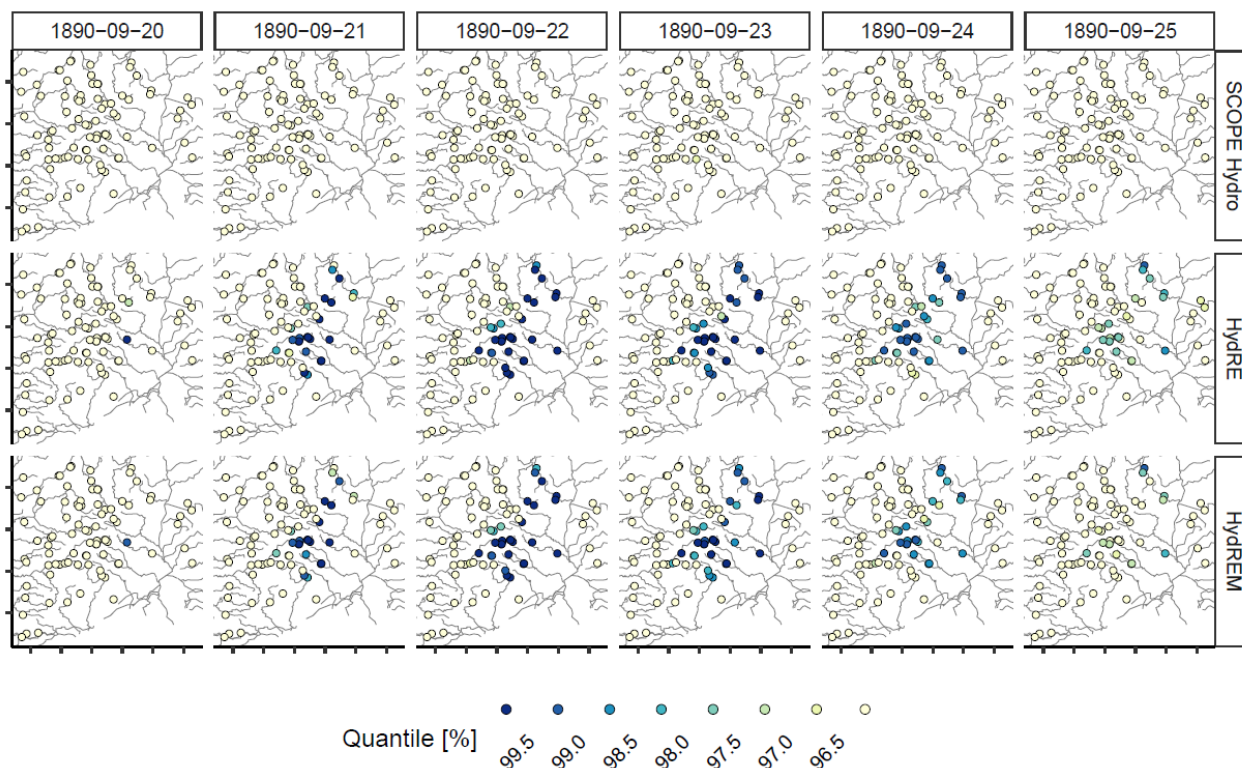
Figure 10. Map of the mean quantiles relative to daily streamflow in the reconstructions over the Cévennes area over 5 days in September 1980.

5 Discussion

5.1 Stability over time

The modeling framework used to produce both HydRE and HydREM is subject to strong assumptions in terms of stability over time.

420   First, the calibration of the hydrological model on a long but yet limited period follows the hypothesis than the link between meteorological and hydrological variables is well captured – even in extrapolation with different hydroclimatic conditions – and that this link is stable over time through a temporal transferability of parameters. Over long periods such as the one considered here, this assumption could be questionable, especially if the calibration is made during a wet or dry period. In our case, even if the calibration is made over 26 years, it seems that, at least for the Seine catchment, a wet phase is present

425   during the whole calibration period (see Figure 8 and Boé and Habets (2014); Bonnet et al. (2020)). A longer calibration period could lead to several hydrological differences, and a solution could be to use the whole period of availability of the observation instead of being limited to 1973-2006. In this regard, some methods could have been used to quantify the sensitivity

of the calibration to the period, such as the classical split-sample test ($Kleme\check{s}$, 1986) but also new methods testing the validity of these assumptions. Two examples are the Generalized Split-Sample Test (Coron et al., 2012) using of calibration-validation periods using a 10 year sliding window, and the Robustness Assessment Test (Nicolle et al., 2021) assessing potential undesirable dependencies of hydrological model performance to climate variables.

Secondly, the stability of the reconstructions also depends on the stability of the input data. For HydRE and HydREM, FYRE Climate is used to forced the GR6J model. This reanalysis is a combination of SCOPE Climate and in-situ measurements of precipitation and temperature. Then some sources of instability can be potentially present : (1) the SCOPE Climate dataset is driven by the Twentieth Century Reanalysis which may include some trend inconsistencies (Krueger et al., 2013), (2) the SCOPE climate used a bais-correction of precipitation based on the 1958-2008 period as reference (Caillouet et al., 2019) that could not be stable over time and, (3) the assimilation of station measurements in FYRE Climate could also lead to temporal inconsistencies due to the evolution of the observation network and of its quality.

5.2 Uncertainty in the modeling/calibration framework

The modelling framework of this study includes several types of uncertainty: (1) the measurement uncertainty during calibration and model error definition, (2) the uncertainty in the input meteorological variables during calibration, simulation and model error definition, and (3) the modelling uncertainty in HydrEM. In order to characterise and account for these uncertainties, we used both a Monte-Carlo approach - through the hypothesis that the uncertainty of these variables can be represented by an ensemble - during the calibration and simulation, and a representation of the errors by a distribution during the application and definition of the error model.

To account for these uncertainties, there are several methods, including the GLUE (Smith et al., 2019) and the Bayesian approach (Renard et al., 2010). The first try to capture all the uncertainty by using a large number of parameter sets and only a few are retained based on the quality of the reconstruction during a recent period. The second also try to quantify a total forecast uncertainty, but by defining input and structural components. While our approach is closer to the Bayesian approach, it clearly differs because, unlike the Bayesian approach, no inference is defined between the input and structural components.

Hence, a logical path to improvement of the modeling framework proposed here would be too applied a proper Bayesian methodology such as the one propose in Renard et al. (2010).

5.3 Definition of the error model

Concerning the error model, an previously developed postprocessing approach has been apply with some modifications to match the ensemble context (see Section 3.5). In this updated version as well as in the the original one, some hypotheses need to be discussed. First, the original approach relies on the assumption that residuals errors (i.e. the ratio of observed streamflow over simulated streamflow) follow a log-normal distribution inside each class defined. This hypothesis allows to transform residuals through a log-transformation to obtain a gaussian distribution defined only with the mean and standard deviation of the residuals. This hypothesis was verified here through histogram checks (not shown here) but this hypothesis could be comforted through the Shapiro Wilk test (Shapiro and Wilk, 1965). Secondly, errors in the HydRE ensemble and

measurements are assumed here to follow a gaussian distribution which is a stong assumption especially for the observations, in that case it would not be right to remove the uncertainty of HydRE nor the observations from the error model (see Eq. 5). Finally, the definition of the model error over a given period (here equal to the calibration period) contain the same assumptions as mentioned in Sect. 5.1. It should be noted that the approach followed to define the error model is not the only one that exists

465 and that a multi-model approach could have been implemented (Arsenault et al., 2015; Thébault et al., 2023).Even if this approach has a higher computational cost, it allows to withdraw the hypothesis of the stability of the error over time.

5.4 On the validation of hydrological and climate data

The validation of HydRE and HydREM was done here through different periods, time scales, spatial scales, and using both observations and other available reconstructions. Still, in the distant past – in our case before 1920 – the validation of the

470 reconstructions is made difficult by the lack of data over a large number of catchments. Finally, a further validation of the HydRE and HydREM could use other hydrological reconstructions covering the 1900–2005 period (Bonnet et al., 2017, 2020). However, those reconstructions provide only streamflow over larger catchments that the ones considered here.

Besides, the reconstructions produced here allow to learn more about the strengths and weaknesses of the FYRE Climate reanalysis used as input. Indeed, as the quality of the hydrological reconstruction depends strongly on the quality of the input

475 (Caillouet et al., 2017; Raimonet et al., 2017; Smith et al., 2019), the hydrological modeling provides an independent validation of FYRE Climate. Thus, this paper shows that FYRE Climate provides a good representation of dry/wet extreme events over the entire period 1871-2012. Furthermore, the reconstruction of precipitation appears to be better than previous products - such as SCOPE Climate - leading to a better correlation in terms of discharge. However, the results also suggest a probable dry bias in the FYRE Climate precipitation before 1940.

480 6 Conclusions

The present study provides long-term reconstructions of daily streamflow over a set of 661 near-natural catchments. Their creation is based on the new FYRE Climate reanalysis (Devers et al., 2021) for temperature and precipitation, the SCOPE Climate reconstruction (Caillouet et al., 2019) for evapotranspiration, and the GR6J lumped continuous rainfall-runoff model (Push-palatha, 2013). Furthermore, an effort has been made to take various sources of uncertainty into account in the calibration and

485 simulation framework, including uncertainties in input, streamflow measurement, and hydrological model. The two resulting 25-member ensemble reconstructions, namely HydRE and HydREM, span the 1871-2012 period at the daily time scale .

In Sect. 4.2, HydrRE and HydREM were first compared to existing hydrological reconstructions, SCOPE Hydro and Safran Hydro (Caillouet et al., 2017) through dependent and independent streamflow measurements over the recent period. The newly produced reconstructions show a stronger correspondence with observations than SCOPE Hydro and a similar one with respect

490 to Safran Hydro. Safran Hydro however spans only the 1958-2012 period and does not provide any information about the uncertainty. Overall, the quality of the HydRE and HydREM reconstructions are close to one another but applying the error model leads to a higher reliability. Section 4.3 pushes further the validation using a set of 20 stations with observations available

over the 1920-2012 period. HydRE and HyDREM better reproduce observed streamflow over the entire period than SCOPE
Hydro. Once again, HydREM shows a better reliability than HydRE. Finally, the variability at annual time scale of HydRE and
495   HydREM is closer to the observations than SCOPE Hydro, but before 1950 a slight dry bias seems to be present.

The study of multidecadal variations in Sect. 4.4 over the 4 main rivers of France have put forward the large differences
between SCOPE Hydro and HydRE/HydREM. The latter show a better agreement with the GRUN reconstructions over the
1915-2000 period but with rather large differences from one basin to another. Lastly, the reconstructions were compared over
a small set of catchments located in the Cévennes area during a well-documented flood event in 1890. HydRE and HydREM
500   provide higher streamflow values than SCOPE Hydro, showing the interest of those two datasets for extreme events.

The various results of these study have put forward the interest of both HydRE and HydREM when comparing to other
existing datasets. Those two 25-member reconstructions make available daily streamflow over 661 near-natural catchments of
France between 1 January 1871 and 29 December 2012. For both, the 25-member ensemble spread reflects the uncertainty
of the reconstructed streamflow. A preference should be given to HydREM as results have put forward its higher reliability.
505   However, as the two products show good results in reproducing observations, long-term variations and flood events, we chose
to provide both through two joined datasets : HydRE (Devers et al., 2023a) and HydREM (Devers et al., 2023b).

Data availability.   HydRE (Devers et al., 2023a) and HydREM (Devers et al., 2023b) are made available as netcdf files on the Recherche
Data Gouv platform. Each dataset comprises 25 netcdf files, one for each ensemble member. Please note that ensemble member #1 of HydRE
is associated to member #1 for HydREM, and so on.

510   *Author contributions.*   AD, JPV, CL, and OV conceptualised the study. AD performed the formal analysis, developed the methodology and
conducted the investigation with support of JPV, CL, and OV. AD wrote the original draft, prepared the visualization and JPV, CL, and OV
reviewed manuscript.

Competing interests.   The authors declare that there are no conflicts of interest regarding this work.

Acknowledgements.   The authors would like to thank Météo-France for providing access to the Safran surface reanalysis.

References

Abaza, M., Anctil, F., Fortin, V., and Turcotte, R.: Sequential streamflow assimilation for short-term hydrological ensemble forecasting, Journal of Hydrology, 519, 2692 – 2706, https://doi.org/https://doi.org/10.1016/j.jhydrol.2014.08.038, 2014.

Allen, R., Pereira, L., Raes, D., and Smith, M.: Guidelines for computing crop water requirements-FAO Irrigation and drainage paper 56, FAO-Food and Agriculture Organisation of the United Nations, Rome, Geophysics, 156, 178, 1998.

Andréassian, V., Lerat, J., Loumagne, C., Mathevet, T., Michel, C., Oudin, L., and Perrin, C.: What is really undermining hydrologic science today?, Hydrological Processes, 21, 2819–2822, https://doi.org/10.1002/hyp.6854, 2007.

Arsenault, R., Gatien, P., Renaud, B., Brissette, F., and Martel, J.-L.: A comparative analysis of 9 multi-model averaging approaches in hydrological continuous streamflow simulation, Journal of Hydrology, 529, 754–767, https://doi.org/https://doi.org/10.1016/j.jhydrol.2015.09.001, 2015.

Berthier, C.-H.: Quantification des incertitudes des débits calculés par un modèle pluie-débit empirique, Master's thesis, Université Paris Sud XI, Paris, https://webgr.irstea.fr/wp-content/uploads/2012/07/2005-BERTHIER-DEA.pdf, 2005.

Bhend, J., Franke, J., Folini, D., Wild, M., and Brönnimann, S.: An ensemble-based approach to climate reconstructions, Climate of the Past, 8, 963–976, https://doi.org/10.5194/cp-8-963-2012, 2012.

Boé, J. and Habets, F.: Multi-decadal river flow variations in France, Hydrology and Earth System Sciences, 18, 691–708, https://doi.org/10.5194/hess-18-691-2014, 2014.

Bonnet, R., Boé, J., Dayon, G., and Martin, E.: Twentieth-Century Hydrometeorological Reconstructions to Study the Multidecadal Variations of the Water Cycle Over France, Water Resources Research, 53, 8366–8382, https://doi.org/10.1002/2017WR020596, 2017.

Bonnet, R., Boé, J., and Habets, F.: Influence of multidecadal variability on high and low flows: the case of the Seine basin, Hydrology and Earth System Sciences, 24, 1611–1631, https://doi.org/10.5194/hess-24-1611-2020, 2020.

Bourgin, F., Ramos, M., Thirel, G., and Andréassian, V.: Investigating the interactions between data assimilation and post-processing in hydrological ensemble forecasting, Journal of Hydrology, 519, 2775 – 2784, https://doi.org/https://doi.org/10.1016/j.jhydrol.2014.07.054, 2014.

Brigode, P., Brissette, F., Nicault, A., Perreault, L., Kuentz, A., Mathevet, T., and Gailhard, J.: Streamflow variability over the 1881-2011 period in northern Québec: comparison of hydrological reconstructions based on tree rings and geopotential height field reanalysis, Climate of the Past, 12, 1785–1804, https://doi.org/10.5194/cp-12-1785-2016, 2016.

Brown, T. A.: Admissible Scoring Systems for Continuous Distributions., Tech. rep., Rand Corp., Santa Monica, CA., https://eric.ed.gov/?id=ED135799, 1974.

Caillouet, L., Vidal, J.-P., Sauquet, E., and Graff, B.: Probabilistic precipitation and temperature downscaling of the Twentieth Century Reanalysis over France, Climate of the Past, 12, 635–662, https://doi.org/10.5194/cp-12-635-2016, 2016.

Caillouet, L., Vidal, J.-P., Sauquet, E., Devers, A., and Graff, B.: Ensemble reconstruction of spatio-temporal extreme low-flow events in France since 1871, Hydrology and Earth System Sciences, 21, 2923–2951, https://doi.org/10.5194/hess-21-2923-2017, 2017.

Caillouet, L., Vidal, J.-P., Sauquet, E., Graff, B., and Soubeyroux, J.-M.: SCOPE Climate: precipitation, https://doi.org/10.5281/zenodo.1299760, 2018a.

Caillouet, L., Vidal, J.-P., Sauquet, E., Graff, B., and Soubeyroux, J.-M.: SCOPE Climate: temperature, https://doi.org/10.5281/zenodo.1299712, 2018b.

Caillouet, L., Vidal, J.-P., Sauquet, E., Graff, B., and Soubeyroux, J.-M.: SCOPE Climate: Penman-Monteith reference evapotranspiration, https://doi.org/10.5281/zenodo.1251843, 2018c.

Caillouet, L., Vidal, J.-P., Sauquet, E., Graff, B., and Soubeyroux, J.-M.: SCOPE Climate: a 142-year daily high-resolution ensemble meteorological reconstruction dataset over France, Earth System Science Data, 11, 241–260, https://doi.org/10.5194/essd-11-241-2019, 2019.

555 Caillouet, L., Jean-Philippe, V., Eric, S., and Alexandre, D.: Safran Hydro, https://doi.org/10.57745/YEZYSF, 2023a.

Caillouet, L., Jean-Philippe, V., Eric, S., and Alexandre, D.: SCOPE Hydro, https://doi.org/10.57745/TCFPHD, 2023b.

Clark, M. P., Rupp, D. E., Woods, R. A., Zheng, X., Ibbitt, R. P., Slater, A. G., Schmidt, J., and Uddstrom, M. J.: Hydrological data assimilation with the ensemble Kalman filter: Use of streamflow observations to update states in a distributed hydrological model, Advances in Water Resources, 31, 1309 – 1324, https://doi.org/https://doi.org/10.1016/j.advwatres.2008.06.005, 2008.

560 Compo, G. P., Whitaker, J. S., Sardeshmukh, P. D., Matsui, N., Allan, R. J., Yin, X., Gleason, B. E., Vose, R. S., Rutledge, G., Bessemoulin, P., Brönnimann, S., Brunet, M., Crouthamel, R. I., Grant, A. N., Groisman, P. Y., Jones, P. D., Kruk, M. C., Kruger, A. C., Marshall, G. J., Maugeri, M., Mok, H. Y., Nordli, Ø., Ross, T. F., Trigo, R. M., Wang, X. L., Woodruff, S. D., and Worley, S. J.: The Twentieth Century Reanalysis Project, Quarterly Journal of the Royal Meteorological Society, 137, 1–28, https://doi.org/10.1002/qj.776, 2011.

Cook, E. R., Seager, R., Kushnir, Y., Briffa, K. R., Büntgen, U., Frank, D., Krusic, P. J., Tegel, W., van der Schrier, G., Andreu-Hayles,
565 L., Baillie, M., Baittinger, C., Bleicher, N., Bonde, N., Brown, D., Carrer, M., Cooper, R., Čufar, K., Dittmar, C., Esper, J., Griggs, C., Gunnarson, B., Günther, B., Gutierrez, E., Haneca, K., Helama, S., Herzig, F., Heussner, K.-U., Hofmann, J., Janda, P., Kontic, R., Köse, N., Kyncl, T., Levanič, T., Linderholm, H., Manning, S., Melvin, T. M., Miles, D., Neuwirth, B., Nicolussi, K., Nola, P., Panayotov, M., Popa, I., Rothe, A., Seftigen, K., Seim, A., Svarva, H., Svoboda, M., Thun, T., Timonen, M., Touchan, R., Trotsiuk, V., Trouet, V., Walder, F., Ważny, T., Wilson, R., and Zang, C.: Old World megadroughts and pluvials during the Common Era, Science Advances, 1,
570 https://doi.org/10.1126/sciadv.1500561, 2015.

Coron, L., Andréassian, V., Perrin, C., Lerat, J., Vaze, J., Bourqui, M., and Hendrickx, F.: Crash testing hydrological models in contrasted climate conditions: An experiment on 216 Australian catchments, Water Resources Research, 48, https://doi.org/https://doi.org/10.1029/2011WR011721, 2012.

Coron, L., Thirel, G., Delaigue, O., Perrin, C., and Andréassian, V.: The suite of lumped GR hydrological models in an R package, Environ-
575 mental modelling & software, 94, 166–171, 2017.

Crooks, S. and Kay, A.: Simulation of river flow in the Thames over 120 years: Evidence of change in rainfall-runoff response?, Journal of Hydrology: Regional Studies, 4, 172 – 195, https://doi.org/https://doi.org/10.1016/j.ejrh.2015.05.014, 2015.

Dayon, G., Boé, J., and Martin, E.: Transferability in the future climate of a statistical downscaling method for precipitation in France, Journal of Geophysical Research: Atmospheres, 120, 1023–1043, https://doi.org/10.1002/2014JD022236, 2015.

580 Devers, A., Vidal, J.-P., Lauvernet, C., Graff, B., and Vannier, O.: A framework for high-resolution meteorological surface reanalysis through offline data assimilation in an ensemble of downscaled reconstructions, Quarterly Journal of the Royal Meteorological Society, 146, 153–173, https://doi.org/10.1002/qj.3663, 2020a.

Devers, A., Vidal, J.-P., Lauvernet, C., and Vannier, O.: FYRE Climate: Precipitation, https://doi.org/10.5281/zenodo.4005573, 2020b.

Devers, A., Vidal, J.-P., Lauvernet, C., and Vannier, O.: FYRE Climate: Temperature, https://doi.org/10.5281/zenodo.4006472, 2020c.

585 Devers, A., Vidal, J.-P., Lauvernet, C., and Vannier, O.: FYRE Climate: a high-resolution reanalysis of daily precipitation and temperature in France from 1871 to 2012, Climate of the Past, 17, 1857–1879, https://doi.org/10.5194/cp-17-1857-2021, 2021.

Devers, A., Jean-Philippe, V., and Claire, L.: Hydrological REconstruction, https://doi.org/10.57745/ONPAUQ, 2023a.

Devers, A., Jean-Philippe, V., and Claire, L.: Hydrological REconstruction with error Model, https://doi.org/10.57745/HG4IB8, 2023b.

Duband, D.: Rainfall-run-off retrospective of extremes droughts since 1860 in Europe (Germany, Italia, France, Rumania, Spain, Switzer-
land), La Houille Blanche, pp. 51–59, https://doi.org/10.1051/lhb/2010041, 2010.

Dubrion, R.: Le climat et ses excés, Feret Eds, 2008.

Evensen, G.: The Ensemble Kalman Filter: theoretical formulation and practical implementation, Ocean Dynamics, 53, 343–367,
https://doi.org/10.1007/s10236-003-0036-9, 2003.

Franke, J., Brönnimann, S., Bhend, J., and Brugnara, Y.: A monthly global paleo-reanalysis of the atmosphere from 1600 to 2005 for studying
past climatic variations, Scientific Data, 4, https://doi.org/10.1038/sdata.2017.76, 2017.

Ghiggi, G., Gudmundsson, L., and Humphrey, V.: G-RUN : Global Runoff Reconstruction, https://doi.org/10.6084/m9.figshare.9228176.v2,
2019a.

Ghiggi, G., Humphrey, V., Seneviratne, S. I., and Gudmundsson, L.: GRUN: an observation-based global gridded runoff dataset from 1902
to 2014, Earth System Science Data, 11, 1655–1674, https://doi.org/10.5194/essd-11-1655-2019, 2019b.

Giuntoli, I., Renard, B., Vidal, J.-P., and Bard, A.: Low flows in France and their relationship to large-scale climate indices, Journal of
Hydrology, 482, 105 – 118, https://doi.org/https://doi.org/10.1016/j.jhydrol.2012.12.038, 2013.

Gupta, H. V., Kling, H., Yilmaz, K. K., and Martinez, G. F.: Decomposition of the mean squared error and
NSE performance criteria: Implications for improving hydrological modelling, Journal of Hydrology, 377, 80–91,
https://doi.org/https://doi.org/10.1016/j.jhydrol.2009.08.003, 2009.

Hersbach, H.: Decomposition of the Continuous Ranked Probability Score for Ensemble Prediction Systems, Weather and Forecasting, 15,
559–570, https://doi.org/10.1175/1520-0434(2000)015<0559:DOTCRP>2.0.CO;2, 2000.

Kim, H., Watanabe, S., Chang, E. C., Yoshimura, K., Hirabayashi, J., Famiglietti, J., , and Oki, T.: Global Soil Wetness
Project Phase 3 Atmospheric Boundary Conditions (Experiment 1) [Data set], Data Integration and Analysis System (DIAS),
https://doi.org/10.20783/DIAS.501, 2017.

Klemeš, V.: Operational testing of hydrological simulation models, Hydrological Sciences Journal, 31, 13–24,
https://doi.org/10.1080/02626668609491024, 1986.

Krueger, O., Schenk, F., Feser, F., and Weisse, R.: Inconsistencies between Long-Term Trends in Storminess Derived from the 20CR Reanal-
ysis and Observations, Journal of Climate, 26, 868–874, https://doi.org/10.1175/JCLI-D-12-00309.1, 2013.

Kuentz, A., Mathevet, T., Gailhard, J., and Hingray, B.: Building long-term and high spatio-temporal resolution precipitation and air tem-
perature reanalyses by mixing local observations and global atmospheric reanalyses: the ANATEM model, Hydrology and Earth System
Sciences, 19, 2717–2736, https://doi.org/https://doi.org/10.5194/hess-19-2717-2015, 2015.

Lang, M. and Coeur, D.: Les inondations remarquables en France – Inventaire 2011 pour la direction Inondation, p. 640, Quae, 2014.

Le Coz, J., Renard, B., Bonnifait, L., Branger, F., and Boursicaud, R. L.: Combining hydraulic knowledge and uncertain
gaugings in the estimation of hydrometric rating curves: A Bayesian approach, Journal of Hydrology, 509, 573 – 587,
https://doi.org/https://doi.org/10.1016/j.jhydrol.2013.11.016, 2014.

Leleu, I., Tonnelier, I., Puechberty, R., Gouin, P., Viquendi, I., Cobos, L., Foray, A., Baillon, M., and Ndima, P.-O.: La refonte du sys-
tème d'information national pour la gestion et la mise à disposition des données hydrométriques, La Houille Blanche, pp. 25–32,
https://doi.org/10.1051/lhb/2014004, 2014.

Lorenz, E. N.: Atmospheric Predictability as Revealed by Naturally Occurring Analogues, Journal of the Atmospheric Sciences, 26, 636–646,
https://doi.org/10.1175/1520-0469(1969)26<636:aparbn>2.0.co;2, 1969.

Moreau, François: Gestion des étiages sévères : l´exemple de la Loire , La Houille Blanche, pp. 70–76, https://doi.org/10.1051/lhb:200404010, 2004.

Naulet, R., Lang, M., Ouarda, T. B. M. J., Coeur, D., Bobée, B., Recking, A., and Moussay, D.: Flood frequency analysis on the Ardèche river using French documentary sources from the last two centuries, Journal of Hydrology, 313, 58–78, https://doi.org/https://doi.org/10.1016/j.jhydrol.2005.02.011, 2005.

Nicolle, P., Andréassian, V., Royer-Gaspard, P., Perrin, C., Thirel, G., Coron, L., and Santos, L.: Technical note: RAT – a robustness assessment test for calibrated and uncalibrated hydrological models, Hydrology and Earth System Sciences, 25, 5013–5027, https://doi.org/10.5194/hess-25-5013-2021, 2021.

Pardé, M.: Inondations en France en 1935 et 1936, Annales de géographie, 260, 113–123, https://doi.org/10.3406/geo.1937.12162, 1937.

Pardé, M.: Les crues dans le bassin du Rhône en décembre 1954 et janvier 1955, Annales de géographie, 363, 448–452, https://www.persee.fr/doc/geo_0003-4010_1958_num_67_363_16988, 1958.

Plumandon, J.-R.: La sécheresse de l'année 1906, La Nature, 1779, 77–78, 1907.

Poli, P., Hersbach, H., Dee, D. P., Berrisford, P., Simmons, A. J., Vitart, F., Laloyaux, P., Tan, D. G. H., Peubey, C., Thépaut, J.-N., Trémolet, Y., Hólm, E. V., Bonavita, M., Isaksen, L., and Fisher, M.: ERA-20C: An Atmospheric Reanalysis of the Twentieth Century, Journal of Climate, 29, 4083–4097, https://doi.org/10.1175/JCLI-D-15-0556.1, 2016.

Pushpalatha, R.: Low-flow simulation and forecasting on French river basins : A hydrological modelling approach, Theses, AgroParisTech, https://pastel.archives-ouvertes.fr/pastel-00912565, 2013.

Quintana-Segui, P., Moigne, P. L., Durand, Y., Martin, E., Habets, F., Baillon, M., Canellas, C., Franchisteguy, L., and Morel, S.: Analysis of Near-Surface Atmospheric Variables: Validation of the SAFRAN Analysis over France, Journal of Applied Meteorology and Climatology, 47, 92–107, https://doi.org/10.1175/2007jamc1636.1, 2008.

Raimonet, M., Oudin, L., Thieu, V., Silvestre, M., Vautard, R., Rabouille, C., and Le Moigne, P.: Evaluation of Gridded Meteorological Datasets for Hydrological Modeling, Journal of Hydrometeorology, 18, 3027–3041, https://doi.org/10.1175/JHM-D-17-0018.1, 2017.

Renard, B., Kavetski, D., Kuczera, G., Thyer, M., and Franks, S. W.: Understanding predictive uncertainty in hydrologic modeling: The challenge of identifying input and structural errors, Water Resources Research, 46, https://doi.org/10.1029/2009WR008328, 2010.

Shapiro, S. S. and Wilk, M. B.: An analysis of variance test for normality (complete samples), Biometrika, 52, 591–611, 1965.

Sheffer, N. A., Enzel, Y., Benito, G., Grodek, T., Poart, N., Lang, M., Naulet, R., and Cœur, D.: Paleofloods and historical floods of the Ardèche River, France, Water Resources Research, 39, https://doi.org/10.1029/2003WR002468, 2003.

Slivinski, L. C.: Historical Reanalysis: What, How, and Why?, Journal of Advances in Modeling Earth Systems, 10, 1736–1739, https://doi.org/10.1029/2018MS001434, 2018.

Slonosky, V. C.: Wet winters, dry summers? Three centuries of precipitation data from Paris, Geophysical Research Letters, 29, 34–1–34–4, https://doi.org/10.1029/2001GL014302, 2002.

Smith, K. A., Barker, L. J., Tanguy, M., Parry, S., Harrigan, S., Legg, T. P., Prudhomme, C., and Hannaford, J.: A Multi-Objective Ensemble Approach to Hydrological Modelling in the UK: An Application to Historic Drought Reconstruction, Hydrology and Earth System Sciences Discussions, 2019, 1–26, https://doi.org/10.5194/hess-2019-3, 2019.

Thébault, C., Perrin, C., Andréassian, V., Thirel, G., Legrand, S., and Delaigue, O.: Multi-model approach in a variable spatial framework for streamflow simulation, EGUsphere, 2023, 1–34, https://doi.org/10.5194/egusphere-2023-569, 2023.

Valéry, A., Andréassian, V., and Perrin, C.: 'As simple as possible but not simple': What is useful in a temperature-based snow-accounting routine? Part 1 - Comparison of six snow accounting routines on 380 catchments, Journal of Hydrology, 517, 1166 – 1175, https://doi.org/10.1016/j.jhydrol.2014.04.059, 2014.

665 Vidal, J.-P., Martin, E., Franchistéguy, L., Habets, F., Soubeyroux, J.-M., Blanchard, M., and Baillon, M.: Multilevel and multiscale drought reanalysis over France with the Safran-Isba-Modcou hydrometeorological suite, Hydrology and Earth System Sciences, 14, 459–478, https://doi.org/10.5194/hess-14-459-2010, 2010.

Warrach-Sagi, K. and Wulfmeyer, V.: Streamflow data assimilation for soil moisture analysis, Geoscientific Model Development, 3, 1–12, https://doi.org/10.5194/gmd-3-1-2010, 2010.

670 Willems, P.: Multidecadal oscillatory behaviour of rainfall extremes in Europe, Climatic Change, 120, 931–944, https://doi.org/10.1007/s10584-013-0837-x, 2013.

Wongchuig, S. C., de Paiva, R. C. D., Siqueira, V., and Collischonn, W.: Hydrological reanalysis across the 20th century: A case study of the Amazon Basin, Journal of Hydrology, 570, 755 – 773, https://doi.org/https://doi.org/10.1016/j.jhydrol.2019.01.025, 2019.